Emerging unitary evolutions in dissipatively coupled systems

C. Arenz[1] and A. Metelmann[2,3]
[1]*Frick Laboratory, Princeton University, Princeton, New Jersey 08544, USA*
[2]*Department of Electrical Engineering, Princeton University, Princeton, New Jersey 08544, USA*
[3]*Dahlem Center for Complex Quantum Systems and Fachbereich Physik, Freie Universität Berlin, 14195 Berlin, Germany*

(Received 13 June 2019; revised manuscript received 8 October 2019; accepted 6 December 2019; published 3 February 2020)

Having a broad range of methods available for implementing unitary operations is crucial for quantum information tasks. We study a dissipative process commonly used to describe dissipatively coupled systems and show that the process can lead to pure unitary dynamics on one part of a bipartite system, provided that the process is strong enough. As a consequence of these findings, we discuss within the framework of quantum control theory how the dissipative process can enable universal control of the considered part, thereby turning parts of the system into a system capable of universal quantum information tasks. We characterize the time scales necessary to implement gates with high fidelity through the dissipative evolution. The considered dissipative evolution is of particular importance since it can be engineered in the laboratory in the realm of superconducting circuits. Based on a reservoir that is formed by a lossy microwave mode we present a detailed study of how our theoretical findings can be realized in an experimental setting.

DOI: 10.1103/PhysRevA.101.022101

I. INTRODUCTION

The implementation of unitary operations lies at the heart of quantum information processing. Quantum simulators and quantum metrology as well as quantum computing schemes and in general state preparation rely on the ability to implement unitary gates with high accuracy. It is therefore highly desirable to have a broad range of methods at hand for meeting that task. Typically unitary gates are implemented through external pulses, such as tailored optical fields and microwave fields [1]. Methods from quantum control theory [2] can be used to determine the set of operations that can be implemented, whereas optimal control theory provides the tools to calculate the corresponding pulses to implement such gates with high accuracy [3], even allowing one to implement gates in the shortest possible time [4]. Over the past years quantum reservoir engineering schemes [5,6], particularly dissipative state preparation [7] and dissipative quantum computing [8], turned out to be a valuable alternative to unitary gate designs. For instance, instead of implementing a sequence of gates in order to carry out some computation, the computational step is entirely encoded in a suitably engineered dissipative process. Moreover, while the general asymptotic behavior of dissipative processes has been analyzed in great detail in [9], a strong dissipative process can also lead to pure unitary dynamics over a subspace that is robust against the process being considered [10–13]. Such decoherence free subspaces [14] can be used to implement gates in a noiseless manner [15,16] and, furthermore, combined with methods from control theory, can turn parts of a system into a system capable of universal quantum computational tasks [17]. However, identifying decoherence free subspaces and engineering dissipative processes yielding a unitary evolution on parts of the system remains challenging.

In this work we show that a dissipative process commonly used to describe dissipatively coupled systems S_1 and S_2 [18–22] can yield a purely unitary evolution on one system, say S_2. In fact, we show that a dissipative process $\mathcal{D}$ described by the Lindblad operator $L = \sqrt{\gamma}(A_1 - i\frac{\eta}{\gamma}B_2)$, where A_1 and B_2 are Hermitian operators on system S_1 and S_2, yields for large γ the same dynamics on system S_2 as a coherent interaction between S_1 and S_2 would. That is,

$$\lim_{\gamma\to\infty} \mathrm{tr}_1\{e^{\mathcal{D}t}(\rho_1 \otimes \rho_2)\} = \mathrm{tr}_1\{U(t)(\rho_1 \otimes \rho_2)U^\dagger(t)\}, \quad (1)$$

where $U(t) = \exp(-itH)$ is the overall unitary evolution generated by the Hamiltonian $H = \eta A_1 B_2$, $\mathrm{tr}_1\{\cdot\}$ denotes the partial trace over system S_1, and ρ_1 and ρ_2 are the initial states of both systems. Consequently, when system S_1 is prepared in an eigenstate of A_1, the overall dissipative evolution yields for $\gamma \to \infty$ a purely unitary dynamics on system S_2 determined by B_2. Such being the case, as represented in Fig. 1, for two systems S_1 and S_2 undergoing an overall purely nonunitary evolution described by $\mathcal{D}$, system S_2 can evolve entirely unitarily provided the dissipative process is strong enough. For the control properties of S_2 this implies that if system S_2 can be additionally steered by some time-dependent fields, system S_2 can become fully controllable, and thus universal for quantum information tasks. We additionally provide criteria that characterize the time scales for implementing unitary gates with high fidelity through the dissipative process.

The presented dissipative evolution is of particular importance since it can be realized in the laboratory using superconducting circuit architectures. Based on a reservoir that is formed by a strongly damped cavity mode, similar to the setting in [23–26], we discuss in detail how our theoretical findings can be experimentally realized.

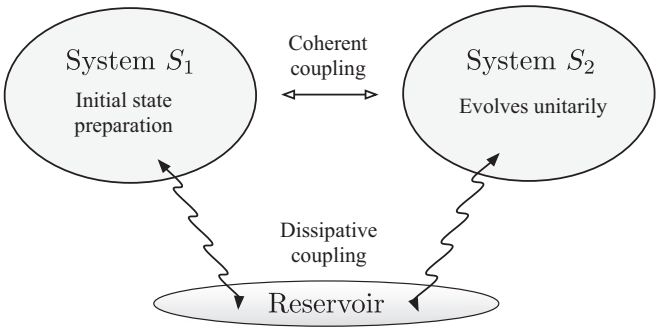

FIG. 1. Schematic representation of two systems S_1 and S_2 that interact coherently described by the Hamiltonian (2) and in a dissipative way described by the Lindblad operator (3) resulting from an interaction with a reservoir. For suitably engineered reservoirs the effect of the coherent interaction on S_2 can be enhanced or suppressed. In fact, if suitably engineered the dissipative process yields the same dynamics for S_2 as the coherent interaction would do [see Eq. (1)]. As such, for certain initial states of S_1, system S_2 evolves unitarily. If additionally system S_2 can be steered by some time-dependent coherent process, the dissipative process can turn system S_2 into a system capable of universal quantum information tasks.

II. DISSIPATIVELY AND COHERENTLY COUPLED SYSTEMS

In order to study the interplay between coherently and dissipatively coupled systems we consider two finite-dimensional systems S_1 and S_2 that interact coherently described by the Hamiltonian

$$H_{\text{coh}} = gA_1B_2, \tag{2}$$

with $A_1 = A \otimes \mathbb{1}_{S_2}$ and $B_2 = \mathbb{1}_{S_1} \otimes B$ being Hermitian operators acting only nontrivially on system S_1 and S_2, respectively, and g being the interaction strength. The two systems are additionally coupled through a reservoir described by the Lindblad operator

$$L = \sqrt{\gamma}\left(A_1 - \frac{\eta}{\gamma}e^{i\phi}B_2\right), \tag{3}$$

so that the evolution of the total system is given by the Lindblad master equation

$$\dot{\rho}(t) = -i[H_{\text{coh}}, \rho(t)] + \mathcal{D}[L](\rho(t)), \tag{4}$$

where ρ is the state of the total system and $\mathcal{D}[L](\rho) = L\rho L^\dagger - \frac{1}{2}(L^\dagger L\rho + \rho L^\dagger L)$ with L given by Eq. (3) is the Lindbladian describing the dissipative process. Here γ denotes the rate associated with the dissipative process for system S_1, while for system S_2 the corresponding rate is η^2/γ ($\eta < \gamma$), reflecting the asymmetric coupling to the dissipation. We remark here that while we start by considering dissipative and coherent interactions together, the coherent interaction is not necessary to obtain purely unitary dynamics on system S_2, as already expressed in Eq. (1). The latter is shown later by focusing on the dissipative part only. Furthermore, at this stage the Lindblad operator is introduced with a general phase ϕ. The master equation then takes the form

$$\dot{\rho}(t) = -i[H_{\text{coh}}, \rho(t)] + \gamma\mathcal{D}[A_1](\rho(t)) + \frac{\eta^2}{\gamma}\mathcal{D}[B_2](\rho(t)) - \mathcal{K}(\rho(t)) + \eta\cos(\phi)\{A_1B_2, \rho(t)\}, \tag{5}$$

with $\{\cdot,\cdot\}$ being the anticommutator and $\mathcal{K}(\rho(t)) = \eta e^{i\phi}B_2\rho(t)A_1 + \text{H.c.}$ From Eq. (5) we immediately see that for $\gamma \to \infty$, which we refer to as the *large* γ *limit*, the dissipative term $\mathcal{D}[B_2]$ on system S_2 vanishes. Moreover, we note that the process $\mathcal{D}[A_1]$ does not affect system S_2. As we will see below, in the large γ limit the term $\mathcal{K}$ can enhance or suppress the coherent interaction depending on the phase ϕ [25,26], as well as give rise to pure unitary dynamics for system S_2.

The evolution of the state $\rho_2(t)$ of system S_2 is given by tracing over system S_1, i.e., $\dot{\rho}_2(t) = \text{tr}_1\{\dot{\rho}(t)\}$. If we evaluate the partial trace in the eigenbasis $\{|\phi_j^{(a)}\rangle\}$ of A with corresponding eigenvalues $\lambda_j^{(a)}$ we find

$$\dot{\rho}_2(t) = -i\sum_j \lambda_j^{(a)}\left\{[g + \eta\,\sin(\phi)]B, \langle\phi_j^{(a)}|\rho(t)|\phi_j^{(a)}\rangle\right\} + \frac{\eta^2}{\gamma}\mathcal{D}[B](\rho_2(t)), \tag{6}$$

from which we see that, depending on the phase ϕ and the effective coherent coupling η, the dissipative interaction can enhance or suppress the effect of the coherent interaction on system S_2. Analogously, the evolution of the state $\rho_1(t)$ of system S_1 is governed by

$$\dot{\rho}_1(t) = -i\sum_j \lambda_j^{(b)}\left\{[g - \eta\,\sin(\phi)]A, \langle\phi_j^{(b)}|\rho(t)|\phi_j^{(b)}\rangle\right\} + \gamma D[A](\rho_1(t)), \tag{7}$$

where $\{|\phi_j^{(b)}\rangle\}$ is the eigenbasis of B with corresponding eigenvalues $\lambda_j^{(b)}$. Notice the sign difference in the commutator part of Eq. (6) and Eq. (7), which leads to unidirectional coherent dynamics due to the dissipative process $\mathcal{D}$. This matches nicely the recipe introduced in Refs. [25,26], where the balancing of a coherent and dissipative process can break the symmetry of reciprocity, rendering an interaction between two systems in a unidirectional fashion. For instance, for $\phi = \pi/2$ and $\eta = g$ the commutator part present in the dynamics of system S_1 vanishes, whereas for system S_2 the part coming from the coherent interaction (2) between both systems is enhanced due to the dissipative process. In addition, under the directionality conditions $\phi = \pi/2$ and $\eta = g$ the full master equation resembles the one obtained from cascaded quantum systems theory [27,28], i.e., the remaining (unidirectional) coupling yields

$$\dot{\rho}(t) \sim i\eta\{[A_1\rho(t), B_2] + [\rho(t)A_1, B_2]\}, \tag{8}$$

affecting only system S_2. However, an important difference to cascaded quantum systems theory here is that one does not require a chiral information transfer via a waveguide to realize such a unidirectional interaction.

We proceed by focusing on the dynamics of system S_2. Assuming the composite system is initially in a product state, one can easily check that in the large γ limit the solution

$\rho_2(t) = \mathcal{E}_t(\rho_2(0))$ to (6) is given by the (bistochastic) completely positive trace preserving (CPTP) map

$$\mathcal{E}_t(\cdot) = \sum_j p_j U_j(t)(\cdot)U_j^\dagger(t), \tag{9}$$

where $p_j = \langle\phi_j^{(a)}|\rho_1(0)|\phi_j^{(a)}\rangle$ with $\rho_1(0)$ being the initial state of system S_1 and the unitaries are given by $U_j(t) = \exp\{-it\lambda_j^{(a)}[g + \eta\ \sin(\phi)]B\}$. For $\phi = \pi/2$ we have $U_j = \exp[-i(\eta + g)\lambda_j^{(a)}B]$ so that the effect of the coherent interaction is enhanced, thereby establishing for $\eta = g$ the equivalence expressed in (1). In the case where $A = \mathbb{1}_{S_1}$ we can already see from the form of the Lindblad operator (3) that $\mathcal{E}_t(\cdot) = U(t)(\cdot)U^\dagger(t)$ with $U(t) = \exp\{-it[g + \eta\ \sin(\phi)]B\}$. For generic Hermitian operators A the preparation of system S_1 in an eigenstate of A yields, up to a modification of B in U by the eigenvalue λ_a, the same unitary map. Furthermore, if in addition to the dissipative process system S_2 is subject to some (possibly time-dependent) coherent process $H_2(t) = \mathbb{1}_{S_1} \otimes H(t)$, in the large γ limit the dynamics of the state $\rho_2(t)$ of system S_2 is governed by the von Neumann equation

$$\dot{\rho}_2(t) = -i\{\lambda_a[g + \eta\ \sin(\phi)]B + H(t), \rho_2(t)\}. \tag{10}$$

In summary, for a suitable choice of the phase in the dissipative process $\mathcal{D}$, the large γ limit enhances or suppresses the effect of the coherent interaction on one part of the bipartite system. Both the large γ limit of the dissipative process given by (3) and the coherent process (2) independently yield the same CPTP map (9) for system S_2. We remark here that the same result can be obtained using a perturbative treatment [13]. If we treat the B_1 term in L as a perturbation to A_1, the unperturbed $\mathcal{D}[A_1]$ effectively yields a (projected) evolution over the decoherence free subspaces of $\mathcal{D}[A_1]$. As shown in [13], if we prepare the system in a decoherence free subspace, the evolution over this subspace can be purely unitary.

In order to investigate the dynamics in more detail, we henceforth focus on the dissipative dynamics given by $\mathcal{D}[L]$ only, where we chose $\phi = \pi/2$ such that

$$L = \sqrt{\gamma}\left(A_1 - i\frac{\eta}{\gamma}B_2\right). \tag{11}$$

We proceed with discussing a few implications of the previous observations. First of all we trivially see that a generic coherent evolution can be created on system S_2 through the dissipative process $\mathcal{D}$. For instance, in the case where system S_2 is given by two noninteracting spins, choosing $B = \sigma_z \otimes \sigma_z$ induces in the γ limit a coherent Ising type interaction. Clearly, the challenge remains to engineer dissipative processes of the form $\mathcal{D}$ containing two-body or many-body interaction terms. Before we address this potential issue by providing a concrete experimental realization based on an engineered reservoir, we want to discuss in the context of quantum control theory how $\mathcal{D}$ can turn the system S_2 into a system capable of universal quantum information tasks. We remark here that this observation immediately follows from the form of Eq. (10) along with standard results in quantum control theory [2], which will be elaborated further in the next section.

A. Universal control

In general the aim of quantum control theory is to steer a quantum system towards a desired target by using a set of suitably tailored classical *control* fields $\{f_k(t)\}$. The total Hamiltonian describing the system reads $H(t) = H_0 + H_c(t)$, where the control typically enters in a bilinear way through $H_c = \sum_{k=1}^n f_k(t)H_k$. We refer to H_0 as the *drift Hamiltonian* and to $\{H_1, \ldots, H_n\}$ as the set of *control Hamiltonians*. The system is said to be *fully controllable* if every unitary transformation $U_g \in \mathrm{SU}(d)$ (for traceless Hamiltonians) with $\mathrm{SU}(d)$ being the group of unitary $d \times d$ matrices with determinant one can be implemented through shaping the control fields $f_k(t)$. It is known that every unitary operation in the closure of the dynamical Lie group $e^{\mathfrak{L}}$ can be implemented with arbitrarily high precision, with $\mathfrak{L} = \mathrm{Lie}(iH_0, iH_1, \ldots, iH_n)$ being the real Lie algebra formed by real linear combinations of the drift and the control Hamiltonians and of their iterated commutators [2]. The system is fully controllable iff $\mathfrak{L} = \mathfrak{su}(d)$, where $\mathfrak{su}(d)$ is the special unitary algebra. That is, every unitary can be implemented up to a global phase arbitrarily well. We remark here that operator controllability implies pure state controllability, i.e., every pure state can be prepared given that the system was initially prepared in a pure state. The dimension of the dynamical Lie algebra $\dim(\mathfrak{L})$ characterizes how *complex* the driven evolution can be [29], and for a fully controllable system of dimension d we have $\dim(\mathfrak{L}) = d^2 - 1$. In [17] it has been shown that a strong dissipative process exhibiting a decoherence free subspace can substantially change the dimension of the dynamical Lie algebra, even turning the system into a fully controllable one. However, this effect critically relies on the ability to arbitrarily control two-body interactions, and, moreover, the increase in $\dim(\mathfrak{L})$ is limited by the dimension of the decoherence free subspace being considered.

In contrast, the strong dissipative process that is determined by the Lindblad operator (11) offers a generic procedure for turning a quantum system through dissipation into a fully controllable one and increasing the dimension of the dynamical Lie algebra arbitrarily. Suppose system S_2 is in addition to the overall acting $\mathcal{D}$ subject to some time varying controls, i.e., the time-dependent Hamiltonian in (10) is given by $H(t) = \sum_{k=1}^n f_k(t)H_k$. Then, in the large γ limit ($\gamma \to \infty$) the unitary operations that can be implemented on system S_2 are determined by the dynamical Lie algebra

$$\mathfrak{L}_{S_2} = \mathrm{Lie}(iB, iH_1, \ldots, iH_n). \tag{12}$$

In the large γ limit the Hermitian operator B given through the Lindblad operator L takes the role of the drift Hamiltonian H_0. Thus the dynamical Lie algebra for system S_2 can be substantially different in the presence of the strong dissipative process $\mathcal{D}$. For instance, in the case of a single control Hamiltonian H_1 on system S_2 the dynamical Lie algebra is just one dimensional if dissipation is absent. Now, if L can be engineered in such a way that B generates together with H_1 the full algebra, i.e., $\mathfrak{L}_{S_2} = \mathfrak{su}(d)$ such that the dynamical Lie algebra has increased from 1 to $\dim(\mathfrak{L}_{S_2}) = d^2 - 1$, system S_2 is turned into a fully controllable system only due to the dissipative process. There are several examples of pairs of Hamiltonians generating the full algebra, for example,

Refs. [30,31], and, moreover, it can be shown that almost all pairs (but a set of measure zero) do the job [32]. Thus system S_2 becomes for almost all choices of B and H_1 fully controllable.

B. Timescales

So far we have studied the time evolution of system S_2 in the large γ limit, i.e., for $\gamma \to \infty$. Now we want to investigate the effect of a finite γ on the fidelity for preparing a state. We consider the fidelity error $\epsilon = 1 - F$, where $F = \langle\psi_G|\rho_2(t)|\psi_G\rangle$ is the fidelity for preparing a pure state $|\psi_G\rangle$ and $\rho_2(t)$ is the state at time t of system S_2. We assume here that system S_2 was initially prepared in a pure state $|\phi(0)\rangle$ such that $|\psi_G\rangle = U|\psi(0)\rangle$ is prepared at time t on system S_2 in the large γ limit.

We begin with the case for which no additional coherent term on system S_2 is present so that the time evolution of system S_2 is entirely determined by the Lindblad operator (11). Since all processes contained in $\mathcal{D}$ mutually commute with each other and assuming that the process $\mathcal{K}$ with $\phi = \pi/2$ prepares the state $|\psi_G\rangle$ at time t, the time evolution of system S_2 is given by $\rho_2(t) = \exp(\frac{\eta^2}{\gamma}\mathcal{D}[B_2]t)(|\psi_G\rangle\langle\psi_G|)$. Expanding $|\psi_G\rangle = \sum_n c_n|\phi_n^{(b)}\rangle$ in the eigenbasis $\{|\phi_n^{(b)}\rangle\}$ of B with corresponding eigenvalues $\{\lambda_n^{(b)}\}$ the fidelity error then reads $\epsilon = 1 - \sum_{n,m}|c_n|^2|c_m|^2\exp[-\frac{t\eta^2}{2\gamma}(\lambda_n^{(b)} - \lambda_m^{(b)})^2]$. We can conclude that we need

$$\frac{\gamma}{\eta^2} \gg \frac{t}{2}\max_{n\neq m}\left(\lambda_n^{(b)} - \lambda_m^{(b)}\right)^2 \tag{13}$$

in order to prepare the state $|\psi_G\rangle$ at time t with high fidelity through the dissipative process.

We proceed with the case in which system S_2 is additionally subject to some possibly time-dependent coherent process described by $H_2(t) = \mathbb{1}_{S_1} \otimes H(t)$, where $H(t)$ could for instance be of the form $H(t) = \sum_{k=1}^{n} f_k(t)H_k$. We saw in the previous paragraph that in this case in the large γ limit every unitary operation $U_g = e^{\Theta}$ with $\Theta \in \mathfrak{L}_{S_2}$ can be implemented on system S_2. Here we now want to study the fidelity error for finite γ for preparing the corresponding state $|\psi_G\rangle = U_g|\psi(0)\rangle$ at time t. Because the relevant processes do not necessarily commute anymore, and moreover the total generator is now time dependent, an exact expression for ϵ as before is not tractable anymore. However, with details found in the Appendix we can upper bound the fidelity error by

$$\epsilon \leqslant \frac{t\eta^2}{2\gamma}(\|B\|_\infty^2 + \|B^2\|_\infty), \tag{14}$$

where $\|\cdot\|_\infty$ is the standard operator norm.

Having discussed the theoretical properties of the dissipative process $\mathcal{D}$, we now turn to presenting an experimental realization of $\mathcal{D}$.

III. EXPERIMENTAL REALIZATION

In general, dissipation is trivially modeled by coupling the system of interest to a Markovian bath. Information is then simply lost into this bath forever and the bath does not mediate any inner correlations in the system. In contrast, engineered dissipation is a controlled form of dissipation; here the system of interest is coupled to a damped auxiliary system which mediates a manipulable dissipative process. Engineering a nonlocal dissipative process of the form $\mathcal{D}[L](\rho)$ between systems S_1 and S_2, with the jump operator L being a combination of Hermitian operators of S_1 and S_2, e.g., Eq. (3), requires both systems to be coupled to a strongly damped auxiliary system in a coherent and controllable manner. The easiest form of such an auxiliary system is a damped mode a. Then the required coherent system-bath dynamics are described by a Hamiltonian of the form

$$H_{\mathrm{SB}} = \lambda_1 X_{\varphi_1} A_1 + \lambda_2 X_{\varphi_2} B_2, \tag{15}$$

with $X_{\varphi_n} = [a\, e^{-i\varphi_n} + a^\dagger e^{i\varphi_n}]$ being the quadrature operators of the a mode. These quadratures X_{φ_n} do not have to be orthogonal, but crucial is their relative phase $\varphi_1 - \varphi_2$, which determines the phase in the resulting nonlocal jump operator L. To have H_{SB} generate the dissipative process $\mathcal{D}[L](\rho)$, we couple mode a to a Markovian bath with rate γ_a. In the case of strong damping, i.e., for $\gamma_a \to \infty$, the auxiliary mode can be adiabatically eliminated [33,34] and one is left with the dissipative process described by the Lindblad operator

$$L = \frac{2\lambda_1}{\sqrt{\gamma_a}}\left[A_1 + \frac{\lambda_2}{\lambda_1}e^{-i(\varphi_1-\varphi_2)}B_2\right]. \tag{16}$$

Thus an asymmetry in the coherent couplings λ_1 and λ_2 translates directly to an asymmetry in the dissipative process between systems S_1 and S_2. And, as mentioned above, the relative phase of the quadratures allows for a finite phase in the nonlocal dissipator. Note that here H_{SB} has to be a resonant interaction, i.e., if the auxiliary mode is detuned, one generates an effective coherent coupling $H_{\mathrm{eff}} \sim A_1B_2$ between systems S_1 and S_2 too.

As discussed in Sec. II, in the large γ limit one can create effective coherent dynamics for system S_2. Crucially, we have to make a distinction here in terms of what we consider large damping. On the one side we have the dissipation of the a mode associated with the rate γ_a. The latter has to be large to obtain L in Eq. (16) out of H_{SB} given in Eq. (15). On the other side, to realize coherent dynamics in S_2 the *engineered* dissipation has to be large, i.e., we have to realize $\eta^2/\gamma \to 0$, while keeping the resulting effective coherent coupling η finite; cf. Eq. (6). By comparing the dissipators given in Eq. (3) and Eq. (16) we identify

$$\gamma = \frac{4\lambda_1^2}{\gamma_a}, \quad \eta = \frac{4\lambda_1\lambda_2}{\gamma_a}. \tag{17}$$

Thus $\eta^2/\gamma \to 0$ is obtained for large γ_a and small coupling λ_2 of system S_2 to the auxiliary mode, which is in agreement with the adiabatic elimination condition $\gamma_a \to \infty$. However, to keep the effective coherent coupling strength η finite, the coupling λ_1 of system S_1 to the auxiliary mode has to compensate for a small ratio λ_2/γ_a, while fulfilling $\lambda_1 < \gamma_a$ to justify the adiabatic elimination. This means that the *engineered* dissipation rate γ, scaling quadratically with λ_1, has to be sufficiently large to obtain the desired unitary dynamics, i.e., in total we require a scaling $\lambda_2 \ll \lambda_1 < \gamma_a \simeq \gamma$.

To illustrate this further we have performed numerical simulation [35] for two qubits coupled via an XX coupling, i.e., we choose $A_1 = \sigma_1^x$ and $B_2 = \sigma_2^x$. In addition, we simulated

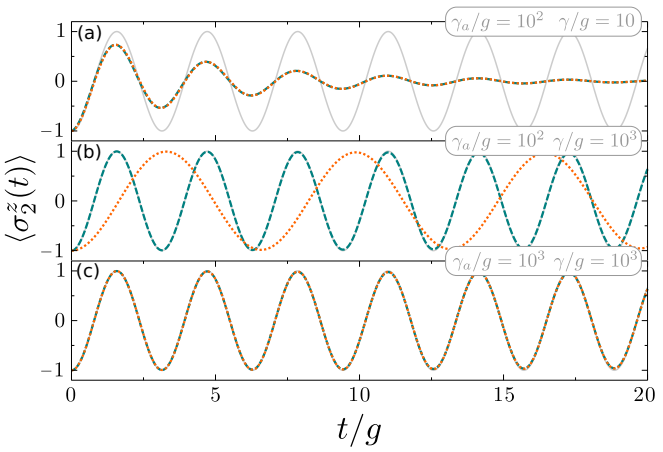

FIG. 2. Rabi oscillations of the expectation of σ_2^z in XX-coupled qubits for different values of the damping rates γ, γ_a (values as denoted in the graphs). The gray solid line depicts the dynamics under the coherent Hamiltonian $H_{xx} = g\sigma_1^x\sigma_2^x$, where qubit 1(2) initially was in an eigenstate of $\sigma_1^x(\sigma_2^z)$. The orange dotted line shows the equivalent dynamics resulting from the system-bath Hamiltonian in Eq. (15) with $A_1 = \sigma_1^x$ and $B_2 = \sigma_2^x$, while the blue dashed line depicts the corresponding dissipative dynamics described by the Lindblad operator Eq. (16). Here, the effective coherent coupling is matched to the coherent coupling, i.e., $\eta = g$, and the remaining parameters can be extracted from $\lambda_1/g = \sqrt{\gamma_a\gamma}/2$ and $\lambda_2/g = \sqrt{\gamma_a/\gamma}/2$.

the dynamics resulting from the corresponding system-bath Hamiltonian Eq. (15) to verify the validity of the adiabatic elimination, assuming the oscillator mode was initially prepared in the vacuum state. As expected, we find that a large γ_a is required for the dynamics of the system-bath Hamiltonian in Eq. (15) to coincide with dissipative dynamics described by the Lindblad operator Eq. (16); cf. Fig. 2(a). When the engineered dissipation rate γ is small compared to the effective coherent coupling η (and therewith the ratio η^2/γ), the resulting dynamics is not unitary as visible in the damped oscillation depicted in Fig. 2(a). Increasing the value of γ fixes this issue and the dissipative dynamics coincides with the evolution resulting from the coherent interaction $H_{xx} = g\sigma_1^x\sigma_2^x$. Crucially, in order to obtain this equivalence expressed in (1), the value of γ_a has to be increased simultaneously; cf. Figs. 2(b) and 2(c). Thus we find that the large damping limit applies to both the dissipation of the auxiliary system (γ_a) and the *engineered* dissipation (γ). Both decay rates have to be of the same order to obtain unitary dynamics of system S_2, i.e., $\gamma_a/g \simeq \gamma/g \gg 1$ has to be fulfilled.

Engineering unitary dynamics in system S_2 via a dissipative process L as given in Eq. (16) can especially be beneficial for realizing higher-order processes. The dissipative process requires a lower order in the system-bath Hamiltonian compared to engineering the higher-order process coherently. This is straightforwardly seen by considering the example of a multipartite system S_1 with N qubits interacting with system S_2 with M qubits such that

$$A_1 = \prod_{n=1}^{N} \sigma_n, \quad B_2 = \prod_{m=1}^{M} \sigma_m, \tag{18}$$

so that the coherent process is of order $N + M$, but if engineered via a dissipator L in Eq. (16) out of H_{SB} given in Eq. (15), the required processes are of order $N + 1$ and $M + 1$, where the $+1$ results from the coupling to the auxiliary mode. Crucially, for $N, M \geqslant 2$ the required processes in H_{SB} are of lower order than the coherent process H_{coh}. Thus, in the large γ limit, the dissipatively engineered higher-order process in system S_2 has been achieved via lower-order processes, and therewith we have mitigated the more challenging engineering of the higher-order process in a coherent manner.

In the following section we present a concrete example of how to realize a nonlocal dissipative process between a three-spin system.

A. Superconducting circuit implementation

Over the past decade, the realm of superconducting circuitry [36–38] has experienced tremendous growth due to advances in nanofabrication technologies, which in turn have led to an impressive progress in the development of quantum technologies. Despite being macroscopic elements, i.e., on the length scale of hundreds of nanometers, superconducting circuits behave quantum mechanically, as they can be designed to be well isolated from the environment. For a recent review, please see Ref. [38].

The basic toolbox of superconducting circuits utilized for quantum simulation and quantum computation consists of linear and nonlinear resonators, where the latter can be operated as artificial few-level atoms or qubits. Superconducting qubits are formed via the two lowest energy states of a nonlinear Kerr resonator. The nonlinearity of the resonator is crucial here for the design of the qubits, as it is accompanied with discrete energy levels which are not equally spaced (in contrast to a linear oscillator). The nonlinear Kerr resonator can be realized by combining a linear LC-resonator circuit with a nonlinear and dissipationless inductance: the Josephson junction. Once placed into a low temperature environment these nonlinear Kerr resonators enter the quantum regime and can be treated as artificial two-level systems also known as qubits. Mixing between multiple qubits can be accomplished via tunable couplers [39–42], and the readout, manipulation, and control of the qubits can be realized via the coupling to the discrete electromagnetic modes of quantum cavities or to the continuum of modes in a waveguide.

In this section we are going to discuss a concrete example on how to engineer a nonlocal dissipative process in a three-qubit system based on a superconducting circuit architecture. We would like to stress that this is just one of many possible realizations and we choose the present setup because it nicely illustrates that one circuit can provide the same type of coherent and dissipative nonlinear process, with the difference that engineering the coherent interaction requires processes that are of higher order than the processes leading to dissipative interactions.

The multiqubit system we would like to consider is formed by three nonlinear Kerr resonators, e.g., a transmission line intersected with a Josephson junction, which are operated in the low excitation and low dissipation regime. For a strong enough Kerr nonlinearity each resonator can be considered as an effective two-level system, which we describe by the Pauli

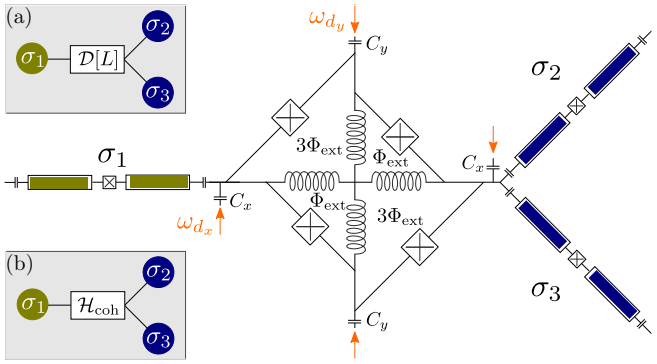

FIG. 3. Three-qubit coupling via a Josephson ring modulator. The resulting interaction between the qubits can be either of the dissipative form (a) $\mathcal{D}[L]$ with $L = \sigma_1 + \sigma_2\sigma_3$ or of the coherent form (b) $H_{\rm coh} = \sigma_1\sigma_2\sigma_3$. The nature of the interaction is determined by the external drives (see text for details).

spin operators σ_n, where $n = 1, 2, 3$ labels each two-level system. To realize a dissipative coupling between the qubits we aim for the situation that all three nonlinear resonators are coupled to the same dissipative reservoir, i.e., an auxiliary mode which is strongly damped via the coupling to a Markovian bath with rate γ_a. We focus on realizing a nonlocal jump operator L of the form given in Eq. (3) with $A_1 = \sigma_1$ and $B_2 = \sigma_2\sigma_3$. As discussed above, such a nonlinear dissipative process is realized via the system-bath Hamiltonian

$$H_{\rm SB} = \frac{\sqrt{\gamma\gamma_a}}{2}\left[X_{\varphi_1}\sigma_1 + \frac{\eta}{\gamma}X_{\varphi_2}\sigma_2\sigma_3\right], \tag{19}$$

with $\varphi_2 - \varphi_1 = \pi + \phi$ and ϕ, η, γ as introduced in Eq. (3). We leave the spin component, i.e., $\sigma_n \to \sigma_n^{x,y,z}$, unspecified for now. To realize the interaction in $H_{\rm SB}$ we use a Josephson ring modulator (JRM) [42], which consists of four identical Josephson junctions embedded in a ring geometry. This device provides three-wave mixing between its three spatial mode amplitudes $\phi_{x,y,z}$ and was originally developed for quantum-limited amplification of weak signals [43]. The whole circuit is sketched in Fig. 3 and can be modeled via the Hamiltonian

$$H = H_0 + \sum_{m=x,y,z}\sum_{n=1}^{3} g_{nm}[d_m\sigma_n^+ + d_m^\dagger\sigma_n^-] + V_{\rm JRM}, \tag{20}$$

where H_0 contains the free energy of the two-level systems and the JRM modes $\phi_m = \phi_{0,m}(d_m + d_m^\dagger)$, where $\phi_{0,m}$ denotes the standard deviation of the zero-point flux fluctuation for the JRM mode ϕ_m. The second term describes excitation exchange between the qubits and the JRM modes with interaction strength g_{nm}, which depend on the design of the coupling capacitors C_m; cf. Fig. 3. $V_{\rm JRM}$ denotes the mixing potential

$$V_{\rm JRM} = -E_J\sum_{\pm}\left[\cos\frac{\phi_x \mp \phi_y}{2\phi_0}\cos\frac{2(2\pm1)\phi_{\rm ext} \pm \phi_z}{2\phi_0}\right] \tag{21}$$

for the spatial mode amplitudes $\phi_{x,y,z}$ realized via the JRM and the latter potential is tunable via the external flux $\phi_{\rm ext}$. E_J denotes the Josephson energy, which is assumed to be identical for all four junctions, and $\phi_0 = \hbar/2e$ corresponds to the reduced flux quantum. We choose a design where the JRM loop is shunted with linear inductors as depicted in Fig. 3. For simplicity we neglect the frequency shifts associated with the potential energies of the inductors. The resulting inner loops of the JRM are asymmetrical biased, i.e., with an external flux $\phi_{\rm ext}(3\phi_{\rm ext})$ for the small (big) loops. Such kind of setup was proposed earlier to realize tunable multibody interactions employed to protect quantum information in cat-code approaches [44] and for quantum annealing protocols [45].

For our purpose we set $\phi_{\rm ext} = \pi/4\phi_0$ and assume that the x mode and y mode are externally driven by multiple pump tones. This external driving ensures that the otherwise far off resonant nonlinear processes are enforced. For now we do not further specify the involved driving frequencies, but make the classical approximation $\phi_x\phi_y \to 4\phi_{0,x}\phi_{0,y}\alpha_x\alpha_y\mathcal{M}(t)$, where $|\alpha_n|^2$ denotes the average photon number in the n-mode induced by the external drives, and the time-dependent modulation is given by

$$\mathcal{M}(t) = \prod_{n=x,y}\sum_{m}\cos\left(\omega_{n,m}^d t + \phi_{n,m}\right), \tag{22}$$

with m drives on each mode with frequencies $\omega_{n,m}^d$; crucially, these drives are associated with the phases $\phi_{n,m}$.

Expanding the JRM mixing potential yields

$$V_{\rm JRM} \approx \frac{E_J\alpha_x'\alpha_y'}{2\sqrt{2}}\mathcal{M}(t)\left[\frac{\phi_z}{\phi_0} - \frac{\phi_z^2}{4\phi_0^2} - \frac{\phi_z^3}{24\phi_0^3}\right], \tag{23}$$

with $\alpha_n' = \alpha_n\phi_{0,n}/\phi_0$. In what follows, the z mode is going to be our auxiliary mode and the choice of the drive frequencies will determine which interactions are resonant in the three-spin system. The frequencies of the circuit should be engineered such that all three qubits are dispersively coupled to the z mode. In this regime we can perform the Schrieffer-Wolff transformation

$$H' = e^{-S}He^S, S = \sum_{n=1}^{3}\lambda_{nz}[d_z^\dagger\sigma_n^- - d_z\sigma_n^+], \tag{24}$$

where $\lambda_{nz} = g_{nz}/\Delta_{nz}$ and Δ_{nz} denotes the detuning of qubit n with respect to the z mode. In the dispersive limit λ_{nz} is small and we only keep terms up to second order in λ_{nz}. In addition, we apply a rotating wave approximation to eliminate fast rotating terms. The remaining effective interaction yields

$$H_{\rm eff} = -\Lambda\,\mathcal{M}(t)(d_z + d_z^\dagger)\left[\lambda_{1z}\,\sigma_1^x + \beta\,\sigma_2^x\sigma_3^x\right], \tag{25}$$

with the coefficients

$$\Lambda = \frac{E_J\alpha_x'\alpha_y'}{\sqrt{2}}\frac{\phi_{z,0}^2}{4\phi_0^2}, \quad \beta = \lambda_{2z}\lambda_{3z}\frac{\phi_{z,0}}{2\phi_0}. \tag{26}$$

The effective interaction Hamiltonian $H_{\rm eff}$ is close to the desired form, cf. Eq. (19), but it is still time-dependent through the modulation $\mathcal{M}(t)$.

This time dependence can be omitted by moving into the right rotating frame and choosing the appropriate driving frequencies. First we move into an interaction frame with respect to the modified free Hamiltonian H_0', i.e., the free-energy part of the Hamiltonian after the Schrieffer-Wolff transformation has been performed. This unitary operation gives us for the spin operators $\sigma_n^x \to \sigma_n^+e^{+i\Omega_n t} + \sigma_n^-e^{-i\Omega_n t}$ and the z-mode operator $d_z \to d_ze^{-i\omega_z t}$, where $\Omega_n(\omega_z)$ is the

(shifted) frequency of qubit n (z mode). Inserting these expressions into the interaction Eq. (25), we can identify the required driving frequencies, e.g., the processes $d_z\sigma_n^{\pm}$ oscillate in this frame with $(\omega_z \pm \Omega_n)$, thus choosing the external modulation at these frequencies renders these processes resonant. Overall, we find six modulation frequencies to obtain the desired operators A_1 and B_2:

$$\begin{aligned} \omega_{1,\pm} &= \omega_z \pm \Omega_1 && \Rightarrow \quad A_1 = \sigma_1^x, \\ \left.\begin{aligned} \omega_{2,\pm} &= \omega_z \pm (\Omega_2 + \Omega_3) \\ \omega_{3,\pm} &= \omega_z \pm (\Omega_2 - \Omega_3) \end{aligned}\right\} && \Rightarrow \quad B_2 = \sigma_2^x\sigma_3^x. \end{aligned} \tag{27}$$

Luckily, the six frequencies $\omega_{n,\pm}$ are asymmetric and antisymmetric combinations of four basic tones; thus an appropriately chosen four-tone driving of the modes x and y is sufficient to produce these six tones; cf. Eq. (22) with $\omega_{n,m}^d$ as the external drive frequencies. To obtain the required modulation frequencies $\omega_{m,\pm}$ $(m = 1, 2, 3)$ it is sufficient to drive the x mode with one tone at $\omega_{x,1}^d = \omega_z$ and the y mode at three different frequencies: $\omega_{y,m}^d = \Omega_1, \Omega_2 \pm \Omega_3$. Setting these frequencies into Eq. (22) and applying basic trigonometric product rules results in the modulation $\mathcal{M}(t) = \mathcal{M}_+(t) + \mathcal{M}_-(t)$ with

$$\mathcal{M}_{\pm}(t) = \frac{1}{2}\sum_{m=1}^{3}\cos\left[\left(\omega_z \pm \omega_{y,m}^d\right)t + \phi_{m,\pm}\right], \tag{28}$$

and with the definition $\phi_{m,\pm} = \phi_{y,m} \pm \phi_{x,1}$. Combining this modulation with the interaction given in Eq. (25), performing a rotating wave approximation, and setting $\phi_{1,+} = \phi_{1,-} \equiv \phi_1$ and $\phi_{2,\pm} = \phi_{3,\pm} \equiv \phi_2$ leaves us with the resonant (time-independent) terms:

$$H_{\text{eff}} \approx -\frac{\Lambda}{4}\left(\lambda_{1z}X_{\phi_1}\sigma_1^x + \beta X_{\phi_2}\sigma_2^x\sigma_3^x\right) \equiv H'_{\text{SB}}, \tag{29}$$

which is of the desired form for the system-bath interaction; cf. Eq. (19). In a last step we assume that the z mode is strongly damped with rate γ_z, so we can adiabatically eliminate it.

Thus, in the large γ_z limit, the discussed circuit design provides the dissipative process for system S_1 and S_2 described by the jump operator

$$L = \frac{\Lambda\lambda_{1z}}{2\sqrt{\gamma_z}}\left(\sigma_1^x + \frac{\beta}{\lambda_{1z}}e^{-i(\phi_1-\phi_2)}\sigma_2^x\sigma_3^x\right). \tag{30}$$

Creating now effective coherent dynamics for system S_2 requires additionally the large γ limit. When mapping the parameters of the dissipator to the ones given in Eq. (3) we find $\phi_2 - \phi_1 = \pi + \phi$ and

$$\gamma = \frac{\Lambda^2}{4\gamma_z}\lambda_{1z}^2, \quad \eta = \frac{\Lambda^2}{4\gamma_z}\frac{\phi_{z,0}}{2\phi_0}\lambda_{1z}\lambda_{2z}\lambda_{3z}. \tag{31}$$

The induced damping η^2/γ of system S_2 scales inversely with the decay rate of the z mode; thus the condition is in good agreement with the requirement of a strongly damped z mode, as expected from the discussion at the beginning of this section. The dispersive coupling strength λ_{1z} of qubit 1 to the z mode has to compensate for a small ratio $\lambda_{2z}\lambda_{3z}/\gamma_z$ to obtain a finite effective coherent coupling strength η. Hence we see here that the large γ limit for this experimental realization is rather a strong dispersive limit, where the hierarchy $\lambda_{2z}\lambda_{3z} \ll \lambda_{1z}$ is the crucial ingredient.

B. Nonreciprocal coherent dynamics

The large γ limit results in coherent dynamics of system S_2 as would have been obtained from $H_{\text{coh}} = gA_1B_2$. As mentioned in Sec. II, having both processes, the dissipative and the coherent one, enables us to render the system directional. The introduced circuit architecture allows as well the realization of a coherent interaction of the form given in Eq. (2). In the dispersive regime we obtain the process

$$H'_{\text{coh}} = -\lambda\mathcal{M}(t)\sigma_1^x\sigma_2^x\sigma_3^x, \quad \lambda = \Lambda\lambda_{1z}\beta, \tag{32}$$

which originates from the cubic term in the V_{JRM} potential given in Eq. (23). This coherent interaction is a third-order process in the dispersive limit, i.e., it scales with $\lambda_{1z}\lambda_{2z}\lambda_{3z}$; in contrast to this, for the (equivalent) dissipative process the second order of the dispersive limit was sufficient.

However, this applies here to the order in the dispersive limit, but not to overall order of the process, i.e., the system-bath Hamiltonian in Eq. (19) requires a third-order process between the z mode and system S_2 and therewith is of the same order as the process in Eq. (32).

Note, considering the cubic term in the potential would in principle require one to perform the Schrieffer-Wolff transformation up to the third order as well, an additional step we have omitted here.

For now we just want to briefly illustrate how the introduced circuit architecture can realize H'_{coh}. The required drive frequencies are obtained by making the substitution $\omega_z \to \Omega_1$ in Eq. (27). Thus we can still work with the same basic tones and just add another drive to the x mode at $\omega_{x,2}^d = \Omega_1$. The total modulation becomes $\mathcal{M}_{\text{tot}}(t) = \mathcal{M}(t) + \mathcal{M}_+^{\text{coh}}(t) + \mathcal{M}_-^{\text{coh}}(t)$ with

$$\mathcal{M}_{\pm}^{\text{coh}}(t) = \frac{1}{2}\sum_{m=1}^{3}\cos\left[\left(\Omega_1 \pm \omega_{y,m}^d\right)t + \theta_{m,\pm}\right], \tag{33}$$

and the phases $\theta_{m,\pm} = \phi_{y,m} \pm \phi_{y,1}$. Note, the modulation $\mathcal{M}_{\text{tot}}(t)$ results as well in an unused tone at $2\Omega_1$, which should not drive any additional process if the involved resonances are designed appropriately. For $\theta_{m,\pm} = \pi$ we obtain the coherent interaction $H'_{\text{coh}} = \lambda/4\ \hat{\sigma}_1^x\hat{\sigma}_2^x\hat{\sigma}_3^x$.

Combining now this coherent process H'_{coh}, and the dissipative process $\mathcal{D}[L](\rho)$ with the jump operator L given in Eq. (30) and $\phi_2 - \phi_1 = \pi + \phi$, the interaction between systems S_1 and S_2 becomes fully nonreciprocal under the conditions [25,26]

$$\phi = \pm\frac{\pi}{2}, \quad \Lambda = \gamma_z, \tag{34}$$

where the sign of the phase determines whether system S_1 or S_2 is affected by the dynamics of the respective other system. For example, for $\phi = \pi/2$ system S_2 performs enhanced coherent dynamics, while system S_1 is not affected; cf. Eq. (6) and Eq. (7).

IV. CONCLUSION

We have analyzed two systems S_1 and S_2 that interact in a coherent and a dissipative way mediated though a reservoir. We showed that the dissipative process can enhance or suppress the effect of the coherent interaction on system S_2. In fact, if suitably engineered, the dissipative process has the same effect on S_2 as the coherent interaction. Consequently, for certain initial states of system S_1, system S_2 evolves unitarily, which implies that if S_2 is additionally steered by some classical time-dependent fields, the dissipative process can allow one to create every unitary gate on S_2. As such, the dissipative process can turn S_2 into a system capable of universal quantum information tasks. Furthermore, based on superconducting circuits, we have presented a scheme to engineer a reservoir that yields the desired dissipative process, as well as the "equivalent" coherent interaction. It is interesting to note that engineering coherent couplings can require processes that are of higher order than the processes leading to dissipative couplings. Given the equivalence of both processes for the dynamics of system S_2, this suggests that engineering the desired dissipation may be more applicable to coherently control one part of a system.

ACKNOWLEDGMENTS

The authors wish to thank V. Albert for useful discussions. A.M. acknowledges funding by the Deutsche Forschungsgemeinschaft through the Emmy Noether program (Grant No. ME 4863/1-1) and the Project No. CRC 910. C.A. acknowledges funding from the Army Research Office (Grant No. W911NF-19-1-0382).

APPENDIX: DERIVATION OF THE UPPER BOUND FOR THE FIDELITY ERROR

Here we derive the upper bound (14) for the fidelity error ϵ in the time-dependent case described by the master equation

$$\dot{\rho}(t) = \mathcal{D}[L](\rho(t)) - i[H_2(t), \rho(t)], \tag{A1}$$

where the Lindblad operator L is given by (3) and $H_2(t) = \mathbb{1}_{S_1} \otimes H(t)$ is a coherent time-dependent process only acting nontrivially on system S_2; assume that no coherent interaction between S_1 and S_2 is present. We set the phase in (3) to $\phi = \pi/2$ and we include the constant η in the operator B acting on S_2. We work in the frame rotating with $H(t)$. That is, we introduce the rotated state $\tilde{\rho} = V^\dagger(t)\rho V(t)$ with $V(t) = \mathcal{T}\exp[-i\int_0^t H(t')dt']$ so that the master equation in the rotated frame reads

$$\dot{\tilde{\rho}}(t) = \mathcal{D}[L(t)](\tilde{\rho}(t)), \tag{A2}$$

where $L(t) = \sqrt{\gamma}[A_1 - i\gamma^{-1}B_2(t)]$ with $B_2(t) = V^\dagger(t)B_2V(t)$, so that

$$\dot{\tilde{\rho}}(t) = \gamma\mathcal{D}[A_1](\tilde{\rho}(t)) + \gamma^{-1}\mathcal{D}[B_2(t)](\tilde{\rho}(t)) - i[B_2(t)\tilde{\rho}(t)A_1 - A_1\tilde{\rho}(t)B_2(t)]. \tag{A3}$$

If system S_1 is initially prepared in an eigenstate $|a\rangle$ of A with corresponding eigenvalue λ_a, in the limit $\gamma \to \infty$ the dynamics of system S_2 is given by the unitary map $\tilde{\mathcal{U}}_t$ generated by $\tilde{\mathcal{H}}_t(\cdot) = -i\lambda_a[B_2(t), \cdot]$. We now want to study the effect of a finite γ by upper bounding the fidelity error $\epsilon = 1 - F$ with $F = \langle\psi_G|\rho_2(t)|\psi_G\rangle$ being the fidelity. We assume that system S_2 is initially prepared in a pure state $|\phi(0)\rangle$ such that in the limit $\gamma \to \infty$ the target state $|\tilde{\psi}_G\rangle$ (in the rotated frame) is prepared on system S_2. That is, if we assume that the initial state of the total system is given by

$$\rho(0) = |a\rangle\langle a| \otimes |\psi(0)\rangle\langle\psi(0)|, \tag{A4}$$

we have $\lim_{\gamma\to\infty} \mathrm{tr}_{S_1}\{\mathcal{T}\, e^{\int_0^t dt'\mathcal{D}[L(t')]}(\rho(0))\} = \tilde{\mathcal{U}}_t(\rho(0)) = |a\rangle\langle a| \otimes |\tilde{\psi}_G\rangle\langle\tilde{\psi}_G|$, whereas for finite γ the state $\tilde{\rho}_2(t)$ in the rotated frame is given by

$$\tilde{\rho}_2(t) = \mathrm{tr}_{S_1}\left\{\mathcal{T}\, e^{\int_0^t dt'\mathcal{D}[L(t')]}(\rho(0))\right\}. \tag{A5}$$

The time order exponential can be written as

$$\mathcal{T}\, e^{\int_0^t dt'\mathcal{D}[L(t')]}(\cdot) = \mathrm{id}(\cdot) + \int_0^t dt_1\mathcal{D}[L(t_1)] + \int_0^t dt_1\int_0^{t_1} dt_2\mathcal{D}[L(t_1)]\circ\mathcal{D}[L(t_2)] + \cdots, \tag{A6}$$

noting that $\mathcal{D}[A_1]$ does not affect system S_2 so that with

$$\mathcal{D}[L(t_1)]\circ\cdots\circ\mathcal{D}[L(t_n)](\rho(0)) = (\mathcal{D}[B_2(t_1)] + \tilde{\mathcal{H}}_{t_1})\circ\cdots\circ(\mathcal{D}[B_2(t_n)] + \tilde{\mathcal{H}}_{t_n})(\rho(0)), \tag{A7}$$

we have

$$\tilde{\rho}_2(t) = \mathrm{tr}_{S_1}\left\{\mathcal{T}\, e^{\int_0^t dt'(\gamma^{-1}\mathcal{D}[B_2(t')] + \tilde{\mathcal{H}}_{t'})}(\rho(0))\right\}. \tag{A8}$$

Defining $\Lambda_t(\cdot) = \mathcal{T}\, e^{\int_0^t dt'\mathcal{L}_{t'}}(\cdot)$ with $\mathcal{L}_t(\cdot) = \gamma^{-1}\mathcal{D}[B_2(t)](\cdot) + \tilde{\mathcal{H}}_t(\cdot)$ we then find

$$\begin{aligned}\|\rho_2(t) - |\psi_G\rangle\langle\psi_G|\|_1 &= \|\,\tilde{\rho}_2(t) - |\tilde{\psi}_G\rangle\langle\tilde{\psi}_G|\|_1 \\ &= \|\mathrm{tr}_{S_1}\{(\Lambda_t - \tilde{\mathcal{U}}_t)(\rho(0))\}\|_1 \\ &\leqslant \|(\Lambda_t - \tilde{\mathcal{U}}_t)(\rho(0))\|_1 \\ &= \|(\tilde{\mathcal{U}}_t^\dagger\circ\Lambda_t - \mathrm{id})(\rho(0))\|_1,\end{aligned} \tag{A9}$$

where we have used that the one norm $\|\cdot\|_1$ is unitarily invariant and $\|\mathrm{tr}_{S_1}\{\cdot\}\|_1 \leqslant \|\cdot\|_1$. In general, the integration of

$$\frac{d}{dt}[(\tilde{\mathcal{U}}_t^\dagger\circ\Lambda_t)(\rho)] = (\tilde{\mathcal{U}}_t^\dagger\circ\tilde{\mathcal{H}}_t^\dagger\circ\Lambda_t + \tilde{\mathcal{U}}_t^\dagger\circ\mathcal{L}_t\circ\Lambda_t)(\rho) \tag{A10}$$

yields

$$\|(\tilde{\mathcal{U}}_t^\dagger\circ\Lambda_t - \mathrm{id})(\rho)\|_1 = \left\|\int_0^t dt'\,\tilde{\mathcal{U}}_{t'}^\dagger\circ(\tilde{\mathcal{H}}_{t'}^\dagger + \mathcal{L}_{t'})\circ\Lambda_{t'}(\rho)\right\|_1, \tag{A11}$$

such that we arrive at

$$\begin{aligned}\|\rho_2(t) - |\psi_G\rangle\langle\psi_G|\|_1 &\leqslant \left\|\int_0^t dt'\,\tilde{\mathcal{U}}_{t'}^\dagger\circ(\tilde{\mathcal{H}}_t^\dagger + \mathcal{L}_{t'})\circ\Lambda_{t'}(\rho(0))\right\|_1 \\ &\leqslant \int_0^t dt'\,\|\tilde{\mathcal{U}}_{t'}^\dagger\circ(\tilde{\mathcal{H}}_{t'}^\dagger + \mathcal{L}_{t'})\circ\Lambda_{t'}(\rho(0))\|_1 \\ &\leqslant \int_0^t dt'\,\|\tilde{\mathcal{U}}_{t'}^\dagger\circ(\tilde{\mathcal{H}}_{t'}^\dagger + \mathcal{L}_{t'})\|_\infty \\ &\leqslant \int_0^t dt'\,\|\tilde{\mathcal{H}}_{t'}^\dagger + \mathcal{L}_{t'}\|_\infty,\end{aligned} \tag{A12}$$

where we used the triangle inequality, again unitary invariance, and $\|S(\rho)\|_1 \leqslant \|S\|_\infty\|\rho\|_1$ valid for some superoperator S with $\|\cdot\|_\infty$ being the standard operator norm. Since $\tilde{\mathcal{H}}_t^\dagger = -\tilde{\mathcal{H}}_t$ we find with the matrix representation of

$\mathcal{D}[B_2(t)]$, obtained from row vectorization of the density operator,

$$\|\rho_2(t) - |\psi_G\rangle\langle\psi_G|\|_1 \leqslant \frac{t}{\gamma}(\|B\|_\infty^2 + \|B^2\|_\infty). \tag{A13}$$

Again, we have used unitary invariance, particularly $\|\tilde{B}(t)\|_\infty = \|B\|_\infty$, and since the fidelity error ϵ is upper bounded by $\frac{1}{2}\|\rho_2(t) - |\psi_G\rangle\langle\psi_G|\|_1$ we have arrived at the desired result (14).

[1] M. A. Nielsen and I. L. Chuang, *Quantum Computation and Quantum Information* (Cambridge University Press, Cambridge, UK, 2010).

[2] D. D'Allesandro, *Introduction to Quantum Control and Dynamics* (Chapman & Hall, New York, 2008).

[3] S. J. Glaser, U. Boscain, T. Calarco, C. P. Koch, W. Köckenberger, R. Kosloss, I. Kuprov, B. Luy, S. Schirmer. T. H. Herbrüggen, D. Sugny, and F. K. Wilhelm, Eur. Phys. J. D **69**, 279 (2015).

[4] T. Caneva, M. Murphy, T. Calarco, R. Fazio, S. Montangero, V. Giovannetti, and G. E. Santoro, Phys. Rev. Lett. **103**, 240501 (2009).

[5] J. F. Poyatos, J. I. Cirac, and P. Zoller, Phys. Rev. Lett. **77**, 4728 (1996).

[6] J. T. Barreiro, M. Müller, P. Schindler, D. Nigg, T. Monz, M. Chwalla, M. Hennrich, C. F. Roos, P. Zoller, and R. Blatt, Nature (London) **470**, 486 (2011).

[7] S. Diehl, A. Micheli, A. Kantian, B. Kraus, H. P. Büchler, and P. Zoller, Nat. Phys. **4**, 878 (2008).

[8] F. Verstraete, M. M. Wolf, and J. I. Cirac, Nat. Phys. **5**, 633 (2009).

[9] B. Baumgartner and H. Narnhofer, J. Phys. A **41**, 395303 (2008).

[10] O. Oreshkov and J. Calsamiglia, Phys. Rev. Lett. **105**, 050503 (2010).

[11] P. Zanardi and L. Campos Venuti, Phys. Rev. Lett. **113**, 240406 (2014).

[12] P. Zanardi and L. Campos Venuti, Phys. Rev. A **91**, 052324 (2015).

[13] V. V. Albert, B. Bradlyn, M. Fraas, and L. Jiang, Phys. Rev. X **6**, 041031 (2016).

[14] D. A. Lidar and T. A. Brun, *Quantum Error Correction* (Cambridge University Press, Cambridge, UK, 2013).

[15] A. Beige, D. Braun, B. Tregenna, and P. L. Knight, Phys. Rev. Lett. **85**, 1762 (2000).

[16] A. Carollo, M. F. Santos, and V. Vedral, Phys. Rev. Lett. **96**, 020403 (2006).

[17] C. Arenz, D. Burgarth, P. Facchi, V. Giovannetti, H. Nakazato, S. Pascazio, and K. Yuasa, Phys. Rev. A **93**, 062308 (2016).

[18] H. Krauter, C. A. Muschik, K. Jensen, W. Wasilewski, J. M. Petersen, J. I. Cirac, and E. S. Polzik, Phys. Rev. Lett. **107**, 080503 (2011).

[19] Y.-D. Wang and A. A. Clerk, Phys. Rev. Lett. **110**, 253601 (2013).

[20] A. Metelmann and A. A. Clerk, Phys. Rev. Lett. **112**, 133904 (2014).

[21] M. E. Kimchi-Schwartz, L. Martin, E. Flurin, C. Aron, M. Kulkarni, H. E. Tureci, and I. Siddiqi, Phys. Rev. Lett. **116**, 240503 (2016).

[22] Y. Liu, S. Shankar, N. Ofek, M. Hatridge, A. Narla, K. M. Sliwa, L. Frunzio, R. J. Schoelkopf, and M. H. Devoret, Phys. Rev. X **6**, 011022 (2016).

[23] B. Vermersch, P. O. Guimond, H. Pichler, and P. Zoller, Phys. Rev. Lett. **118**, 133601 (2017).

[24] Z. L. Xiang, M. Zhang, L. Jiang, and P. Rabl, Phys. Rev. X **7**, 011035 (2017).

[25] A. Metelmann and A. A. Clerk, Phys. Rev. X **5**, 021025 (2015).

[26] A. Metelmann and A. A. Clerk, Phys. Rev. A **95**, 013837 (2017).

[27] C. W. Gardiner and P. Zoller, *Quantum Noise* (Springer, Berlin, 2004).

[28] H. J. Carmichael, Phys. Rev. Lett. **70**, 2273 (1993).

[29] D. K. Burgarth, P. Facchi, V. Giovannetti, H. Nakazato, S. Pascazio, and K. Yuasa, Nat. Commun. **5**, 5173 (2014).

[30] C. Arenz, G. Gualdi, and D. Burgarth, New J. Phys. **16**, 065023 (2014).

[31] S. G. Schirmer, I. C. H. Pullen, and P. J. Pemberton-Ross, Phys. Rev. A **78**, 062339 (2008).

[32] C. Altafini, J. Math. Phys. **43**, 2051 (2002).

[33] H. J. Carmichael, *Statistical Methods in Quantum Optics 2: Non-Classical Fields* (Springer-Verlag, Berlin, 2008).

[34] B. D. Hauer, A. Metelmann, and J. P. Davis, Phys. Rev. A **98**, 043804 (2018).

[35] J. R. Johansson, P. D. Nation, and F. Nori, Comput. Phys. Commun. **183**, 1760 (2012).

[36] A. Blais, R.-S. Huang, A. Wallraff, S. M. Girvin, and R. J. Schoelkopf, Phys. Rev. A **69**, 062320 (2004).

[37] M. H. Devoret and R. J. Schoelkopf, Science **339**, 1169 (2013).

[38] X. Gu, A. F. Kockum, A. Miranowicz, Y.-X. Liu, and F. Nori, Phys. Rep. **718-719**, 1 (2017).

[39] P. Roushan, C. Neill, A. Megrant, Y. Chen, R. Babbush, R. Barends, B. Campbell, Z. Chen, B. Chiaro, A. Dunsworth *et al.*, Nat. Phys. **13**, 146 (2017).

[40] Y. Chen, C. Neill, P. Roushan, N. Leung, M. Fang, R. Barends, J. Kelly, B. Campbell, Z. Chen, B. Chiaro *et al.*, Phys. Rev. Lett. **113**, 220502 (2014).

[41] F. Lecocq, L. Ranzani, G. A. Peterson, K. Cicak, R. W. Simmonds, J. D. Teufel, and J. Aumentado, Phys. Rev. Appl. **7**, 024028 (2017).

[42] N. Bergeal, R. Vijay, V. E. Manucharyan, I. Siddiqi, R. J. Schoelkopf, S. M. Girvin, and M. H. Devoret, Nat. Phys. **6**, 296 (2010).

[43] N. Bergeal, F. Schackert, M. Metcalfe, R. Vijay, V. E. Manucharyan, L. Frunzio, D. E. Prober, R. J. Schoelkopf, S. M. Girvin, and M. H. Devoret, Nature (London) **465**, 64 (2010).

[44] M. Mirrahimi, Z. Leghtas, V. V. Albert, S. Touzard, R. J. Schoelkopf, L. Jiang, and M. H. Devoret, New J. Phys. **16**, 045014 (2014).

[45] S. Puri, C. K. Andersen, A. L. Grimsmo, and A. Blais, Nat. Commun. **8**, 15785 (2017).